MOLECULAR AND CELLULAR BIOLOGY, May 2010, p. 2353–2364 Vol. 30, No. 10
0270-7306/10/$12.00 doi:10.1128/MCB.00116-10

Separable Functions of the Fission Yeast Spt5 Carboxyl-Terminal Domain (CTD) in Capping Enzyme Binding and Transcription Elongation Overlap with Those of the RNA Polymerase II CTD▽

Susanne Schneider,[1,3] Yi Pei,[2] Stewart Shuman,[1,2]* and Beate Schwer[1,3]*

Graduate Program in Molecular Biology, Weill Cornell Medical College, New York, New York 10065[1]; Molecular Biology Program, Sloan-Kettering Institute, New York, New York 10065[2]; and Department of Microbiology and Immunology, Weill Cornell Medical College, New York, New York 10065[3]

Received 29 January 2010/Returned for modification 1 March 2010/Accepted 4 March 2010

An interaction network connecting mRNA capping enzymes, the RNA polymerase II (Pol II) carboxyl-terminal domain (CTD), elongation factor Spt5, and the Cdk7 and Cdk9 protein kinases is thought to comprise a transcription elongation checkpoint. A crux of this network is Spt5, which regulates early transcription elongation and has an imputed role in pre-mRNA processing via its physical association with capping enzymes. *Schizosaccharomyces pombe* Spt5 has a distinctive CTD composed of tandem nonapeptide repeats of the consensus sequence ^{1}TPAWNSGSK^{9}. The Spt5 CTD binds the capping enzymes and is a substrate for threonine phosphorylation by the Cdk9 kinase. Here we report that deletion of the *S. pombe* Spt5 CTD results in slow growth and aberrant cell morphology. The severity of the *spt5-ΔCTD* phenotype is exacerbated by truncation of the Pol II CTD and ameliorated by overexpression of the capping enzymes RNA triphosphatase and RNA guanylyltransferase. These results suggest that the Spt5 and Pol II CTDs play functionally overlapping roles in capping enzyme recruitment. We probed structure-activity relations of the Spt5 CTD by alanine scanning of the consensus nonapeptide. The T1A change abolished CTD phosphorylation by Cdk9 but did not affect CTD binding to the capping enzymes. The *T1A* and *P2A* mutations elicited cold-sensitive (cs) and temperature-sensitive (ts) growth defects and conferred sensitivity to growth inhibition by 6-azauracil that was exacerbated by partial truncations of the Pol II CTD. The *T1A* phenotypes were rescued by a phosphomimetic *T1E* change but not by capping enzyme overexpression. These results imply a positive role for Spt5 CTD phosphorylation in Pol II transcription elongation in fission yeast, distinct from its capping enzyme interactions. Viability of yeast cells bearing both Spt5 CTD *T1A* and Pol II CTD *S2A* mutations heralds that the Cdk9 kinase has an essential target other than Spt5 and Pol II CTD-Ser2.

Eukaryal mRNA processing is linked physically and temporally to transcription elongation. The earliest processing step is mRNA capping, which can occur as soon as the 5′ triphosphate terminus of the nascent RNA extrudes from elongating RNA polymerase (6, 15). The cellular RNA capping enzymes are directed to nascent mRNAs by binding to the phosphorylated carboxyl-terminal domain (CTD) of the largest subunit of RNA polymerase II (Pol II) (7, 8, 18, 34, 29, 57). The Pol II CTD, consisting of tandem heptapeptide repeats of the consensus sequence $Y^1S^2P^3T^4S^5P^6S^7$, functions as a landing pad for diverse cellular proteins that regulate the initiation, elongation, and termination steps of Pol II transcription, modify chromatin structure, and catalyze or regulate RNA capping, splicing, and polyadenylation (30, 37). The inherently plastic CTD structure is sculpted by cyclin-dependent kinases (Cdks) that have various positional specificities and act at different stages of the transcription cycle. The Cdk7 kinase (a component of transcription factor TFIIH) acts at or shortly after initiation to install Ser5-PO_4 and Ser7-PO_4 marks on the CTD (1), of which Ser5-PO_4 is a critical determinant of capping enzyme recruitment and mRNA capping *in vivo* (20, 22, 49).

Capping enzymes may also access the transcription complex by binding to the Pol II elongation factor Spt5 (32, 52). Spt5 is a large polypeptide (~1,000 to 1,200 amino acids [aa]) composed of multiple domain modules, including a distinctive C-terminal repeat domain (the "Spt5 CTD") that directly binds RNA capping enzymes and is targeted for threonine phosphorylation by the Cdk9 protein kinase (33, 56). Spt5 exerts both negative and positive effects on transcription elongation (2, 17, 21, 39, 44, 50, 55). For example, metazoan Spt5 elicits an elongation arrest at promoter-proximal sites that is alleviated by the Cdk9 subunit of P-TEFb (positive transcription elongation factor b) (50, 51). Cdk9 phosphorylates the Pol II CTD and the Spt5 CTD. Studies with analog-sensitive kinase mutants implicate the Spt5 CTD as a *bona fide* substrate for Cdk9 (or its budding yeast ortholog Bur1) (26, 49, 58). Whereas interactions of the capping enzyme with the Spt5 CTD are independent of CTD phosphorylation (in contrast to the capping enzyme/Pol II CTD interactions) (32), the conversion of Spt5 from a negative to a positive elongation mode requires Spt5 CTD phosphorylation by Cdk9 (5, 56).

In the fission yeast *Schizosaccharomyces pombe*, the essential

* Corresponding author. Mailing address for Stewart Shuman: Sloan-Kettering Institute, Molecular Biology Program, 1275 York Ave., New York, NY 10021. Phone: (212) 639-7145. Fax: (212) 772-8410. E-mail: s-shuman@ski.mskcc.org. Mailing address for Beate Schwer: Department of Microbiology and Immunology, Weill Cornell Medical College, 1300 York Ave., New York, NY 10065. Phone: (212) 746-6518. Fax: (212) 746–8587. E-mail: bschwer@med.cornell.edu.

▽ Published ahead of print on 15 March 2010.

Cdk9 kinase exists as a stable heterotrimeric complex *in vivo* with its cyclin partner Pch1 and the mRNA cap methyltransferase Pcm1 (13, 33, 36). *S. pombe* Cdk9 also interacts with Pct1, the RNA triphosphatase component of the capping apparatus (35). In turn, Pct1 and Pce1 (the guanylyltransferase component of the fission yeast capping system) bind directly and independently to the unphosphorylated Spt5 CTD and the phosphorylated Pol II CTD (32, 34). These interactions and others noted above underlie the proposal of a transcription elongation checkpoint that ensures a temporal window for capping of nascent mRNAs (27, 35, 36, 45).

The checkpoint model is attractive insofar as there is evidence that positive and negative regulation of transcription can occur at the step of capping enzyme recruitment (6, 12) and that either diminished cap guanylylation activity or defective installation of the guanylyltransferase-recruiting Ser5-PO_4 Pol II CTD mark can result in the production of uncapped transcripts that suffer premature 5′ exonucleolytic decay (20, 41). However, recent studies highlight that the putative checkpoint is either not enforced or not required on a large fraction of cellular transcription units. For example, genetic or pharmacological inhibition of Cdk9 or Spt5 exerts fairly narrow effects on the levels of certain mRNAs, rather than a global transcriptional dyscrasia (24, 25, 49). One explanation for the limited impact of such inhibition is that there is functional overlap built into the systems that coordinate transcription elongation and mRNA capping. One potential source of functional overlap is the independent interactions of the capping enzymes with the Pol II and Spt5 CTDs.

S. pombe Spt5 and its CTD are the focus of the present study. Spt5 is essential for cell growth in fission yeast (32), as it is in budding yeast and in human somatic cells (24, 47). The 990-aa *S. pombe* Spt5 protein consists of an acidic N-terminal domain, central NusG-like NGN and KOW domains, and an exceptionally regular CTD (aa 801 to 990) composed of tandem repeats of the consensus nonapeptide $T^1P^2A^3W^4N^5S^6G^7S^8K^9$ (see Fig. 2). *S. pombe* Spt5 forms a stable heterodimeric complex with the 105-aa *S. pombe* Spt4 protein (42). The Spt4-docking site on Spt5 is localized to a trypsin-resistant segment from aa 218 to 381 (42). The Spt4-binding module is conserved in *Saccharomyces cerevisiae* and human Spt5, wherein it adopts a compact tertiary structure composed of a central antiparallel β-sheet flanked by three α-helices (14, 16, 53). A genetic analysis of Spt4 in *S. pombe* revealed it to be inessential for growth at 25 to 30°C but critical at 37°C (42). Thus, the unconditionally essential Spt5 protein must be performing Spt4-independent functions. Initial insights into functional compartmentalization of Spt5 emerged from studies of the effects of partial deletions of its CTD nonamer repeat array. As few as three nonamer repeats sufficed for normal *S. pombe* growth, but only when Spt4 was present (42). Synthetic lethality of an *spt5*$^{1\text{-}835}$ *spt4*Δ double mutant at 34°C suggested that interaction of Spt4 with the central domain of Spt5 overlaps functionally with the Spt5 CTD.

Here we have studied the consequences of complete deletion of the Spt5 CTD repeat array, which results in slow growth and aberrant cell morphology. The *spt5-ΔCTD* phenotype is enhanced by truncating the Pol II CTD and suppressed by overexpressing capping enzymes. These results suggest that the Spt5 and Pol II CTDs play functionally overlapping roles in capping enzyme recruitment in fission yeast. We illuminated structure-activity relations in the Spt5 CTD by position-specific alanine scanning. The effects of Thr1 and Pro2 mutations on growth and 6-azauracil sensitivity suggest a positive role for Spt5 CTD phosphorylation in transcription elongation that overlaps elongation functions of the Pol II CTD.

MATERIALS AND METHODS

Deletion of the Spt5 CTD in fission yeast. pUC19-based plasmids used for integration of *ura4*$^+$ or *kanMX* markers downstream of *spt5-(1-800)* were constructed as follows. An *spt5* gene fragment extending from an internal NdeI site (at nucleotide +1736) to nucleotide +2400 of the *spt5* open reading frame (ORF) was amplified by PCR using a reverse primer that introduced a stop codon at +2401 and a flanking BamHI site. The DNA fragment was restricted and inserted upstream of the *ura4* and *kanMX* genes in plasmids pUC19-ura4-spt5$^{3'}$ and pUC19-kanMX-spt5$^{3'}$ (42). The spt5$^{\Delta C5'}$-ura4-spt5$^{3'}$ and spt5$^{\Delta C5'}$-kanMX-spt5$^{3'}$ integration cassettes (which contain the flanking 534-bp genomic DNA fragment 3′ of the native *spt5* stop codon) were excised and transformed into a diploid *S. pombe* strain. Ura$^+$ or Geneticin-resistant transformants were selected, and diagnostic Southern blotting was used to verify targeted insertion into the chromosomal *spt5* locus. The heterozygous diploids were then sporulated, and tetrads were dissected to obtain *spt5-(1-800)*::*ura4*$^+$ or *spt5-(1-800)*::*kanMX* haploids, referred to herein as *spt5-ΔC* strains.

Missense mutations of the Spt5 CTD array. CTD cassettes composed of tandem repeats of the wild-type nonamer consensus peptide or a T1A, P2A, W4A, N5A, K9A, or T1E variant were constructed as follows. Pairs of complementary 27-mer 5′-phosphorylated DNA oligonucleotides were designed that, when annealed, consisted of a 23-bp duplex with 5′ GATC overhangs, the sense strand of which encodes either the wild-type peptide GSKTPAWNS or the mutant peptides GSKAPAWNSGS (T1A), GSKTAAWNSGS (P2A), etc. (oligonucleotide sequences are available on request). Reactions of the annealed oligonucleotides with DNA ligase generated concatameric arrays of the repeating units, either in a tail-to-head orientation encoding a tandem nonapeptide repeat or in unfruitful tail-to-tail and head-to-head orientations. The tail-to-tail ligation events generate a BamHI cleavage site (5′-GGATCC) at the junctions, while the head-to-head junctions generate a BglII site (5′-AGATCT). In contrast, the in-frame junctions (5′-GGATCT) are resistant to BamHI and BglII. The ligation products were digested with BamHI and BglII and then resolved by PAGE. Resistant DNA fragments of ~200 bp were isolated from the gels and then ligated into the BamHI site of pHis$_{10}$Smt3, which had been modified to contain a translation stop codon immediately downstream of the BamHI site. DNA sequencing established the continuity of the ORFs, the number of nonapeptide repeats (either 7 or 8 in the constructs used here), and the desired wild-type or mutated amino acid sequences of each repeat.

***S. pombe* strains with Spt5 CTD missense mutations.** The wild-type and mutated Spt5 CTD cassettes were PCR amplified from the respective pHis$_{10}$Smt3-(CTD)$_{7\text{-}8}$ plasmid templates with primers designed to introduce BglII and SmaI sites at the 5′ and 3′ ends, respectively. The PCR products were digested with BglII and SmaI and then fused to the *spt5-(1-800)* ORF of a pDS474-based plasmid (10) by ligation between an engineered BglII site and a filled-in BamHI site that flanked the stop codon. The resulting plasmids were named pDS472-Spt5-(CTD)$_7$, pDS472-Spt5-(T1A)$_7$, etc. Cassettes for integration of the mutated *spt5* alleles into *S. pombe* were constructed by restricting these plasmids with NdeI (at nucleotide +1736 of the *spt5* ORF) and SmaI (in the pDS472 vector) and inserting the ~860-bp CTD-encoding fragments upstream of the *ura4* gene in the pUC19-ura4-spt5$^{3'}$ plasmid. The spt5CTD$^{5'}$-ura4-spt5$^{3'}$ integration cassettes were excised and transformed into *S. pombe* cells. Ura$^+$ transformants were selected and analyzed by diagnostic Southern blotting to verify correct integration.

Truncations of the *S. pombe* Rpb1 CTD array. To generate C-terminal truncations of Rpb1, we first constructed pUC19-natMX-rpb1$^{3'}$, a plasmid containing the *natMX* gene upstream of a 552-bp segment of *S. pombe* genomic DNA 3′ of the *rpb1*$^+$ stop codon. We then inserted upstream of *natMX* a series of *rpb1* gene fragments extending from an EcoRI site (at nucleotide +4086 in the *rpb1*$^+$ ORF) to a newly created stop codon at position +4816, +4858, +4879, +4900, +4921, +4984, +5086, or +5194 that truncated the Rpb1 CTD to 8, 10, 11, 12, 13, 16, 20, or 26 heptads, respectively. Excised rpb1$^{\Delta CTD5'}$-natMX-rpb1$^{3'}$ DNA fragments were introduced into diploid *S. pombe* cells. Transformants were selected on yeast extract with supplements (YES) agar medium containing 0.1 mg/ml

nourseothricin (clonNAT; Werner Bioagents), and the targeted insertions were verified by diagnostic Southern blotting. The heterozygous *rpb1*$^+$/*rpb1-ΔCTD* diploids were then sporulated, and tetrads were dissected.

Combining Spt5 CTD deletion with Rpb1 CTD truncations. *spt5-(1-800)*::*ura4*$^+$ (*h*$^+$) cells were mixed with each of the *rpb1-ΔCTD*::*natMX* (*h*$^-$) strains (*rpb1-26*, *rpb1-20*, *rpb1-16*, *rpb1-13*, and *rpb1-12*) on mating/sporulation agar (11), and the plates were incubated for 2 to 3 days at 30°C. We then dissected 5 to 20 tetrads for each cross and germinated the haploids on YES medium at 30°C. Their genotypes were determined to identify ura$^+$ nat^R double mutants. Whereas tetrad dissection did yield the *spt5-ΔC rpb1-26* and *spt5-ΔC rpb1-20* strains, no viable ura$^+$ nat^R haploids were isolated during tetrad dissections for the other crosses. To screen a larger number of haploid progeny, we performed random spore analysis (11). After plating ~500 spores (determined by counting) on YES agar to determine the percentage that were viable, we plated 3,000 to 8,000 viable spores to selective medium lacking uracil and containing nourseothricin.

Rpb1 CTD-S2A mutant. The *S. pombe rpb1-12xS2ACTD* strain was kindly provided by Jim Karagiannis, University of Western Ontario (23). Genomic DNA was isolated, and a 950-bp C-terminal segment of the *rpb1-12xS2ACTD* strain was amplified by PCR using a forward primer that annealed upstream of the EcoRI site at position +4086 within the *rpb1* ORF and a reverse primer that introduced an XbaI site downstream of the stop codon in the *rpb1-12xS2ACTD* strain. The gene segment was restricted and inserted into pUC19. To expand the S2A repeat domain, we restricted pUC19-rpb1$^{(12xS2A)5'}$ with AarI (at the site corresponding to nucleotide position +4703 within the *rpb1*$^+$ ORF) and AvaI (at a site 16 nucleotides downstream of the AarI site in pUC19-rpb1$^{(12xS2A)5'}$) and inserted therein a short duplex DNA that was generated by annealing two oligonucleotides (5′-ATG CCC TCT TCC CCA TCC TAC GCA CCA ACT TCA CCA TCT TAT GCT CCG ACT TCC and 5′-T CGG GGA AGT CGG AGC ATA AGA TGG TGA AGT TGG TGC GTA GGA TGG GGA AGA GG). The resulting plasmid was named pUC19-rpb1$^{(14xS2A)5'}$. The 990-bp EcoRI/XbaI fragment encoding the modified CTD was excised from pUC19-rpb1$^{(14xS2A)5'}$ and cloned into pUC19-term-natMX-rpb1$^{3'}$, a modified version of pUC19-natMX-rpb1$^{3'}$, in which a 320-bp DNA segment from the *S. cerevisiae TPI1* transcription termination/polyadenylation signal had been inserted upstream of the *natMX* gene. In parallel, the pUC19-based plasmid for integration of *rpb1-16* was modified to contain the *TPI1* termination/polyadenylation signal. The integration cassettes were excised and transformed into haploid *S. pombe* strains to obtain nourseothricin-resistant *rpb1-S2A* and *rpb1-16t* cells.

Combining the Rpb1-S2A and Rpb1-16 variants with Spt5 CTD mutations. The linear rpb1$^{(14xS2A)5'}$-term-natMX-rpb1$^{3'}$ integration cassette was introduced into homozygous *spt5-(CTD)*$_7$/*spt5-(CTD)*$_7$, *spt5-T1A*/*spt5-T1A*, and *spt5-T1E*/*spt5-T1E* diploids, and nourseothricin-resistant transformants were selected. The resulting *rpb1*$^+$/*rpb1-S2A* diploid strains were then sporulated, and tetrads were dissected to obtain the *rpb1-S2A spt5-(CTD)*$_7$, *rpb1-S2A spt5-T1A*, and *rpb1-S2A spt5-T1E* haploid strains that were Ura$^+$ and nourseothricin resistant. A set of control strains containing the same *spt5-CTD* alleles in the *rpb1-16* background (which has a truncated Rbp1 CTD array composed of wild-type heptads) was generated by introducing the linear rpb1$^{(1-16)5'}$-term-natMX-rpb1$^{3'}$ integration cassette into the *spt5-(CTD)*$_7$, *spt5-T1A*, and *spt5-T1E* haploids and selecting for nourseothricin-resistant transformants. Correct targeting of the *rpb1* locus in each case was confirmed by colony PCR and diagnostic Southern blotting.

Recombinant Pce1 and Pct1 proteins. The Pce1 and Pct1 ORFs were PCR amplified from templates p132-PCE1 and pG1-PCT1 (34) with oligonucleotide primers that introduced BamHI and XhoI sites adjacent to the start and stop codons, respectively. The PCR fragments were restricted and inserted into plasmid pGEX-2TKN (Pharmacia) to yield expression plasmids encoding Pce1 and Pct1 fused to an N-terminal GST (glutathione-*S*-transferase) domain. The pGEX-Pct1 and pGEX-Pce1 plasmids were transformed into *Escherichia coli* BL21(DE3) Codon Plus (Novagen). Cultures derived from single transformants were maintained in logarithmic growth in LB medium containing 100 μg/ml ampicillin until the A_{600} of a 250-ml culture reached ~0.7. The cultures were chilled on ice for 30 min, adjusted to 0.4 mM isopropyl-β-D-thiogalactopyranoside (IPTG) and 2% (vol/vol) ethanol, and then incubated for 16 h at 17°C with constant shaking. Cells were harvested by centrifugation and stored at −80°C. All subsequent procedures were performed at 4°C. Thawed bacteria were resuspended in 12.5 ml of PBS (50 mM potassium phosphate, pH 7.2, 150 mM NaCl). The suspensions were adjusted to 0.2 mg/ml lysozyme and incubated for 45 min. Triton X-100 was added to a final concentration of 0.1%, and incubation was continued for 15 min. The cell suspensions were sonicated to reduce viscosity, and insoluble material was removed by centrifugation for 30 min at 13,000 rpm in a Sorvall SS34 rotor. The soluble extracts were mixed for 1 h with 0.5 ml of glutathione-Sepharose 4B resin (Pharmacia Biotech) that had been equilibrated in PBS. The resins were recovered by centrifugation, suspended in PBS, and poured into a column. The columns were washed twice with 10-ml aliquots of PBS and then eluted with 5 ml of 10 mM glutathione in PBS. The eluates were dialyzed against buffer D (50 mM Tris-HCl, pH 8.0, 100 mM NaCl, 1 mM dithiothreitol [DTT], 10% glycerol, 0.05% Triton X-100) and then stored at −80°C. The protein concentrations were determined by SDS-PAGE analysis of aliquots of the GST-Pce1 and GST-Pct1 polypeptides in parallel with increasing amounts of a bovine serum albumin (BSA) standard solution of known concentration. The gel was stained with Coomassie blue dye, and the staining intensities of GST-Pce1, GST-Pct1, and BSA were quantified with a Molecular Imager ChemiDoc densitometry system. The concentrations of the GST-Pce1 and GST-Pct1 polypeptides were determined by interpolation to the BSA standard curve. The yields of GST-Pce1 and GST-Pct1 from 250-ml bacterial cultures were ~7 mg of each protein.

Recombinant Spt5-CTD proteins. The wild-type and mutated His$_{10}$-Smt3-Spt5-(CTD)$_{7-8}$ plasmids (see above) were transformed into *Escherichia coli* BL21-Codon Plus (DE3). Cultures derived from single colonies were maintained in logarithmic growth in LB medium with 50 μg/ml kanamycin until the A_{600} of a 250-ml culture reached 0.6 to 0.8. The cultures were then placed on ice for 30 min and adjusted to 0.4 mM IPTG and 2% (vol/vol) ethanol before incubation was continued for 16 h at 17°C with constant shaking. Cells were harvested by centrifugation and stored at −80°C. All subsequent procedures were carried out at 4°C. The thawed cell pellets were resuspended in 12.5 ml of buffer A (50 mM Tris-HCl, pH 7.4, 10% sucrose, 250 mM NaCl). The cells were lysed, and soluble extracts were prepared as described above for the recombinant capping enzymes. The soluble lysates were mixed for 1 h with 1 ml of nickel-nitrilotriacetic acid (Ni-NTA)-agarose (Qiagen) that had been equilibrated with buffer A. The resins were recovered by centrifugation, suspended in 10 ml of buffer E (50 mM Tris HCl, pH 7.4, 250 mM NaCl, 10% glycerol) containing 25 mM imidazole, and then poured into columns. The columns were washed twice with 5-ml aliquots of the same buffer, and the bound proteins were then eluted stepwise with 3-ml aliquots of buffer E containing 300 and 500 mM imidazole. The elution profiles were monitored by SDS-PAGE. The 300 mM imidazole eluates containing the His$_{10}$-Smt3-CTD polypeptides were dialyzed against buffer D. Protein concentrations were determined by SDS-PAGE and quantification of staining intensities as described above for the capping enzymes. The yields of His$_{10}$-Smt3-CTD polypeptides recovered from 250 ml bacterial cultures were as follows: 8 mg (wild type), 6 mg (T1A variant), 10 mg (W4A variant), 6 mg (N5A variant), and 4.8 mg (K9A variant).

Binding of Pce1 to Spt5-CTD. His$_{10}$-Smt3-Spt5-CTD proteins (8 μg) were mixed with 8 μg of GST-Pce1 in 50 μl of buffer F (50 mM Tris-HCl [pH 7.4], 10% glycerol) containing 25 mM imidazole. Aliquots were removed to assess "input" material, and the samples were then mixed with 50 μl of a 5% slurry of magnetic Ni-NTA-agarose resin (Qiagen) in buffer F with 25 mM imidazole. The suspensions were incubated for 1 h at 4°C, after which the resins were collected and held at the bottoms of the tubes in a magnetic separator (Qiagen) while the supernatants containing unbound proteins were removed. The resins were washed twice with 500 μl of buffer F with 25 mM imidazole. The bound proteins were then eluted in 30 μl of 500 mM imidazole in buffer F.

Binding of Pct1 to Spt5-CTD. His$_{10}$-Smt3-Spt5-CTD proteins (8 μg) were mixed with 8 μg of GST-Pct1 in 50 μl of buffer E with 25 mM imidazole. Aliquots were removed to assess input material, and the samples were then mixed with 50 μl of a 5% slurry of magnetic Ni-NTA-agarose resin in buffer E with 25 mM imidazole. The suspensions were incubated for 1 h at 4°C, after which the resins were collected and held at the bottoms of the tubes in a magnetic separator while the supernatants containing unbound proteins were removed. The resins were washed twice with 500 μl of buffer E with 25 mM imidazole. The bound proteins were then eluted in 30 μl of 500 mM imidazole in buffer E.

Microscopy. Microscopy was performed using live cells from exponentially growing liquid cultures of *S. pombe*. Cells were harvested by centrifugation, washed in water, and resuspended in water at ~1 A_{600} unit/ml. Aliquots (5 μl) were applied to positively charged slides (Unifrost Plus; Azer Scientific). The yeast cells were visualized and photographed with a Nikon Eclipse E600 microscope (100× objective) coupled to an RT Slider Spot camera. The lengths of individual cells were measured by drawing a bar along the axis of each cell using the Spot Advanced software program (version 4.5).

Western blot analysis. The haploid *spt5*$^+$, *spt5-ΔC*, and various *spt5-(1-800)-(CTD)*$_{7-8}$ strains were maintained in exponential growth in YES medium at 30°C. Aliquots of cells from exponentially growing cultures (containing equivalent A_{600} units) were harvested, and whole-cell extracts were prepared and subjected to SDS-PAGE and immunoblotting with affinity-purified rabbit anti-Spt5 antibodies as described previously (42). The immune complexes were visualized with horseradish peroxidase-conjugated anti-rabbit immunoglobulin using an en-

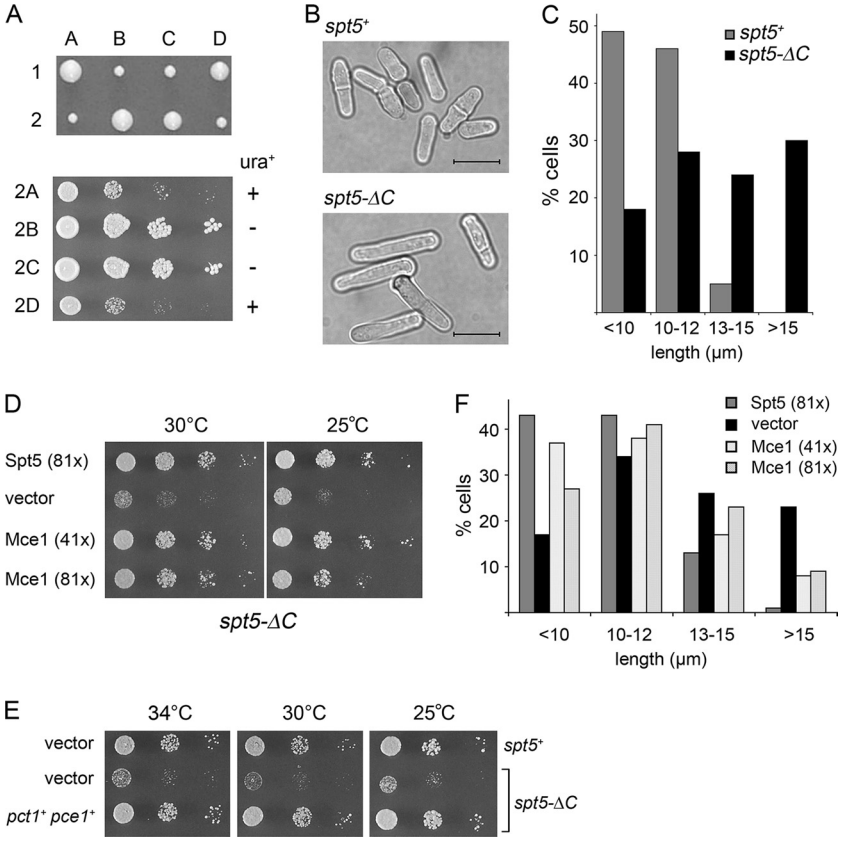

FIG. 1. Deletion of the Spt5 CTD affects cells growth and morphology. (A) Heterozygous spt5$^+$/*spt5-(1-800)*::*ura4*$^+$ diploids were sporulated, and asci were dissected. Individual spores (A, B, C, and D) from two tetrads (1 and 2) were germinated on YES agar at 30°C for 4 days (upper panel). The four haploid progeny of tetrad 2 were grown in liquid culture. The cultures were diluted to attain an A_{600} of 0.1, and aliquots (3 μl) of serial 10-fold dilutions were spotted on YES agar medium. The plates were photographed after incubation for 3 days at 30°C (lower panel). The *spt5*-Δ*C* haploids 2A and 2D are ura$^+$; the *spt5*$^+$ haploids 2B and 2C are ura$^-$. (B) *spt5*$^+$ and *spt5*-Δ*C* cells grown in YES medium at 30°C were examined by light microscopy. Bars, 10 μm. (C) The lengths of 270 *spt5*$^+$ cells and 330 *spt5*-Δ*C* cells were measured and sorted into length bins as specified. The percentage of cells in each bin is represented in a bar graph. (D) Dosage suppression of the *spt5*-Δ*C* phenotype by mammalian capping enzyme Mce1. *spt5*-Δ*C*[*spt5-(1-800)*::*ura4*$^+$] cells were transformed with *LEU2* plasmids as specified. Serial dilutions of *spt5*-Δ*C* strains harboring a pREP81x-Spt5 plasmid (positive control), an empty vector plasmid (negative control), or plasmids for expression of Mce1 under the transcriptional control of an intermediate-strength (41x) or a low-strength (81x) *nmt* promoter were spotted on Leu$^-$ agar medium. The plates were photographed after incubation for 6 days at 25°C or 3 days at 30°C. (E) Dosage suppression of *spt5*-Δ*C* by fission yeast capping enzymes. The *spt5*$^+$ and *spt5*-Δ*C* [*spt5-(1-800)*::*kanMX*] strains harbored two plasmids marked with *ura4*$^+$ and *LEU2*, respectively. These were either empty vector plasmids or plasmids for expression of *S. pombe pct1*$^+$ (RNA triphosphatase) and *pce1*+ (RNA guanylyltransferase) under the transcriptional control of the low-strength *nmt* (81x) promoter. Cultures were grown at 30°C in minimal medium lacking uracil and leucine. Aliquots (3 μl) of serial 10-fold dilutions were spotted on Ura$^-$ Leu$^-$ agar medium and incubated at 25°C (4 days), 30°C (3 days), or 34°C (3 days) as specified. (F) Overexpression of Mce1 partially rescues the elongated phenotype of *spt5*-Δ*C* cells. The lengths of 300 to 500 individual cells were measured. The percentages of cells in each of the four size categories are represented by vertical bars.

hanced chemiluminescence system. Where specified, the blot was stripped and reprobed with anti-PSTAIRE (Cdc2p34) antibody (Santa Cruz Biotechnology), which served as a cell extract loading control.

RESULTS

The Spt5 CTD is important for normal cell growth. The CTD of *S. pombe* Spt5 comprises 18 nonamer repeats of the consensus sequence TPAWNSGSK (Fig. 2). To determine whether the CTD is important for *spt5*$^+$ function *in vivo*, we introduced *spt5-(1-800)*::*ura4*$^+$ into diploid cells so as to replace one copy of *spt5*$^+$ with an allele encoding Spt5-ΔC, a variant that lacks the entire CTD. Ura$^+$ haploids were recovered upon sporulation and dissection of *spt5*$^+$/*spt5-(1-800)*::*ura4*$^+$ cells, indicating that the Spt5 CTD is not essential for viability (Fig. 1A). However, the CTD is important for normal cell growth, insofar as *spt5*-Δ*C* cells formed smaller colonies than *spt5*$^+$ sisters on YES agar at 30°C (Fig. 1A). The growth defect of *spt5*-Δ*C* cells on agar medium was also evident at 18°C, 20°C, 25°C, 32°C, 34°C, and 37°C (Fig. 1D and E; see also Fig. 4D). The doubling time of *spt5*-Δ*C* cells in YES liquid medium at 30°C was 3.5 h, *versus* 2.1 h for *spt5*$^+$ cells (not shown).

We observed that cells lacking the Spt5 CTD were elongated compared to wild-type cells (Fig. 1B and C and Fig. 2). Whereas 49% and 46% of *spt5*$^+$ cells grown in YES medium at 30°C were <10 μm and 10 to 12 μm, respectively, only 18% and 28% of the *spt5*-Δ*C* cells fell in these two categories. Thirty percent of *spt5*-Δ*C* cells were >15 μm (Fig. 1C), including

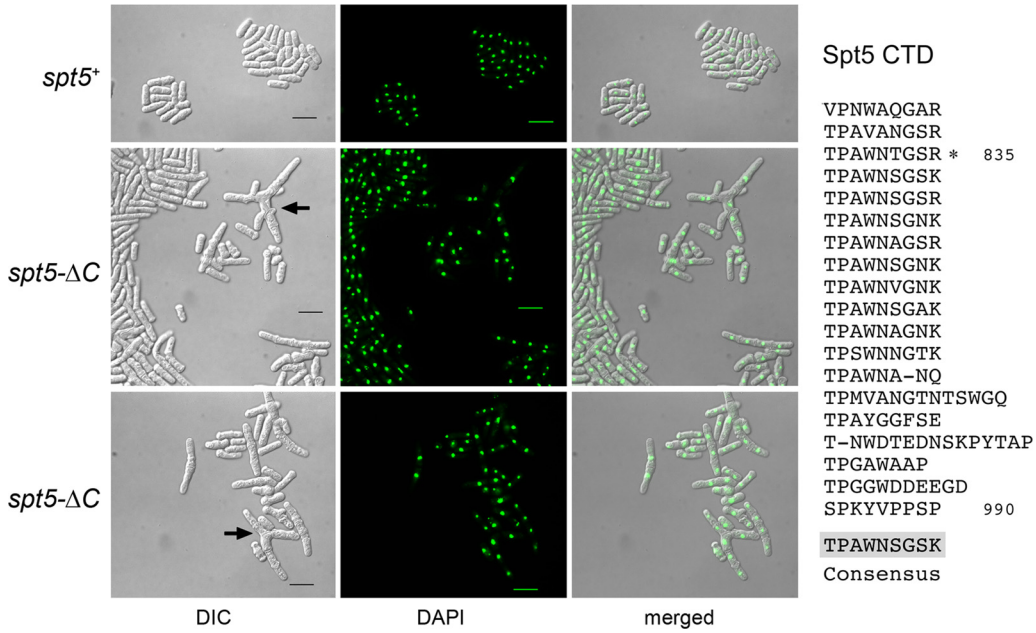

FIG. 2. Deletion of the Spt5 CTD results in aberrant cell morphology. The amino acid sequence of the Spt5 CTD is displayed at right, with the nonamer repeats aligned vertically. The consensus sequence TPAWNSGSK is shown below the alignment. Previously it was shown that truncation of the CTD to amino acid 835, leaving three nonamer repeats, had no apparent impact on cells growth. In the present study, the entire CTD was deleted in the *spt5*-Δ*C* strains of *S. pombe*. Cell morphology and nuclear DNA localization were assessed by light microscopy. *spt5*$^+$ and *spt5*-Δ*C* cells were cultured in YES medium at 30°C. Exponentially growing cells were fixed in 70% ethanol, treated with 4′,6-diamidino-2-phenylindole (DAPI), and then visualized by differential interference contrast (DIC) and fluorescence (DAPI) microscopy (Nikon Eclipse E600 microscope equipped with a Spot camera). The bars in the DIC images are 10 μm. The arrows denote branched cells.

hyperelongated cells (>20 μm) and cells with branches and multiple septa (Fig. 2). We conclude that the absence of the CTD results in slow growth and abnormal cell morphology.

Overexpression of capping enzymes alleviates the growth phenotype of *spt5-ΔC* cells. The fission yeast mRNA capping enzymes Pct1 (RNA triphosphatase) and Pce1 (RNA guanylyltransferase) bind directly to the Spt5 CTD (32). If the recruitment of capping enzymes to the transcription complex is impaired in the absence of the Spt5 CTD, then overexpression of capping enzymes might suppress some of the *spt5*-Δ*C* phenotypes. We introduced into *spt5*-Δ*C* cells a multicopy plasmid for expression of the mammalian capping enzyme Mce1—a bifunctional triphosphatase-guanylyltransferase that binds avidly to the phosphorylated Pol II CTD (18)—under the control of the medium-strength (41x) and low-strength (81x) *nmt1* promoters (9). Growth was assessed by spotting aliquots of serial dilutions of the cell cultures onto agar medium and incubating the plates at 25°C and 30°C. *spt5*-Δ*C* cells that had been transformed with a plasmid expressing Spt5 under the control of the 81x promoter served as a positive control. We found that cells harboring *MCE1* plasmids grew as well as the Spt5 control cells, as gauged by colony size (Fig. 1D). *nmt1*-driven overexpression of both fission yeast capping enzymes (Pct1 plus Pce1) on multicopy plasmids also suppressed the slow-growth phenotype of *spt5*-Δ*C* cells (Fig. 1E). Furthermore, overexpression of Mce1 partially reversed the morphological defects of *spt5*-Δ*C* cells, insofar as only 8 to 9% of *MCE1* cells were >15 μm long, compared to 23% of *spt5*-Δ*C* cells harboring the vector plasmid (Fig. 1F). In the suppressed strains, no branched or multiseptated cells were observed (not shown). These findings suggest that recruitment of the capping enzymes to the transcription complex is compromised in the absence of the Spt5 CTD, and we infer that dosage suppression is a consequence of increased binding of the capping enzymes to Pol II, likely via the Rpb1 CTD.

Functional overlap of the Spt5 and Pol II CTDs. The CTD of the *S. pombe* Pol II large subunit Rpb1, which consists of 29 heptad repeats of the consensus sequence YSPTSPS (4) (Fig. 3), binds directly to Pct1 and Pce1 (34) and thus provides an alternative docking site for the capping enzymes on the Pol II elongation complex, potentially buffering the impact of deleting the Spt5 CTD. If so, we reasoned that deleting a portion of the Rpb1 CTD might exacerbate the growth defect of *spt5*-Δ*C*. The effects of incremental shortening of the Pol II CTD have been studied extensively in budding yeast (31, 54), yielding powerful genetic insights into transcriptional control mechanisms (48). The role of Pol II CTD length in *S. pombe* has received comparatively little attention (23).

Here we integrated a series of *rpb1*-Δ*CTD*::*natMX* alleles into the *rpb1*$^+$ locus in diploid cells, so as to express Rbp1 variants with 26, 20, 16, 13, 12, 11, 10, or 8 heptad repeats (named *rpb1-26*, *rpb1-20*, etc.) (Fig. 3). By sporulating the diploids and characterizing the haploid progeny, we established a clear hierarchy of CTD length effects on cell growth. For example, eight heptad repeats were lethal, i.e., we never recovered nourseothricin-resistant haploids after sporulation of *rpb1*$^+$/*rpb1-8* diploids. *rpb1-10* cells were viable, but they grew poorly at 30°C and failed to form colonies at 20°C or 37°C (Fig. 3A). *rpb1-11*, *-12*, and *-13* cells showed gradually improved growth at the low and high temperatures. The *rpb1-16*,

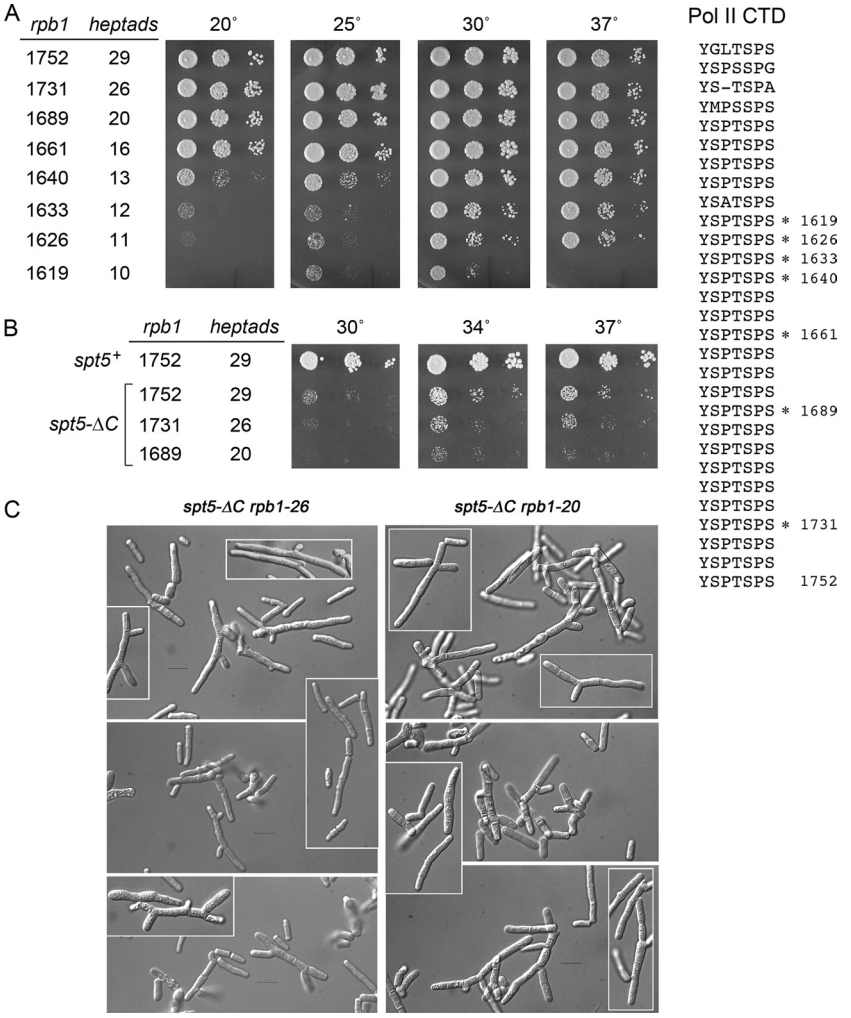

FIG. 3. Genetic interactions of *rpb1-ΔCTD* mutants with *spt5-ΔC*. The amino acid sequence of the *S. pombe* Rpb1 CTD (aa 1551 to 1752) is shown at right; the 29 heptapeptide repeats are stacked vertically. The C termini of the *rpb1-ΔCTD* mutants are indicated by asterisks. (A) Truncating the Rpb1 CTD impairs growth. *S. pombe* strains bearing the indicated *rpb1* alleles were tested for growth on YES agar. Aliquots of serial 5-fold dilutions of cultures that had been adjusted to an A_{600} of 0.1 were spotted onto YES agar and incubated at the indicated temperatures. The plates were photographed after incubation for 7 days at 20°C, 4 days at 25°C, 3 days at 30°C, or 2 days at 37°C. *rpb1* alleles are named according to the length of the Rpb1 protein variants; the numbers of heptad repeats are indicated. (B) Phenotypic enhancement of *rpb1-ΔCTD* mutations by *spt5-ΔC*. Viable haploid double mutants harboring *spt5-ΔC* and the indicated CTD truncations of *rpb1* were analyzed by spotting on YES agar. The plates were photographed after incubation for 3 days at 30, 34, or 37°C. (C) Aberrant morphology of *spt5-ΔC rpb1-ΔCTD* double mutants. Aliquots of exponentially growing cultures were spotted on slides, and the cells were visualized by differential interference contrast microscopy. All images, including the highlighted inserts, were taken at the same magnification. Bars, 10 μm.

rpb1-20, and *rpb1-26* strains grew as well as the *rpb1*$^+$ strain at all temperatures tested (Fig. 3A). These results indicate that 16 heptad repeats comprise a fully active Pol II CTD in fission yeast. Overexpression of Mce1 had no salutary effect on the conditional growth defects of the *rpb1-10*, *-11*, *-12*, and *-13* strains (not shown), suggesting that additional Pol II functions were perturbed by these CTD truncations.

To illuminate genetic interactions between the Pol II and Spt5 CTDs, we analyzed haploid progeny from genetic crosses between the *spt5-ΔC* strain and several of the *rpb1-ΔCTD* mutants. The *rpb1-26 spt5-ΔC* and *rpb1-20 spt5-ΔC* double mutants were recovered at the expected frequencies (20 to 25% of all spores analyzed). However, these strains were sicker than the *spt5-ΔC* single mutant at 30 to 37°C (Fig. 3B) and failed to form colonies at lower temperatures (data not shown). Light microscopy inspection of *rpb1-26 spt5-ΔC* and *rpb1-20 spt5-ΔC* cells grown in liquid culture at 30°C revealed a high percentage with elongated and aberrant shapes (Fig. 3C).

Genetic crosses between the *spt5-ΔC* strain and the *rpb1-16* or *rpb1-13* strain yielded double mutants that comprised ~9% and ~0.15%, respectively, of all haploid progeny, signifying progressive synthetic interactions with CTD-less Spt5 as the Pol II CTD was shortened below a critical threshold. Indeed, the rare surviving *rpb1-13 spt5-ΔC* strains could not be propagated when restreaked, and the *rpb1-16 spt5-ΔC* strain formed microscopic colonies only (data not shown). Finally, we failed to recover any *rpb1-12 spt5-ΔC* double mutants among ~4,500 haploid progeny screened. These findings of synthetic lethality

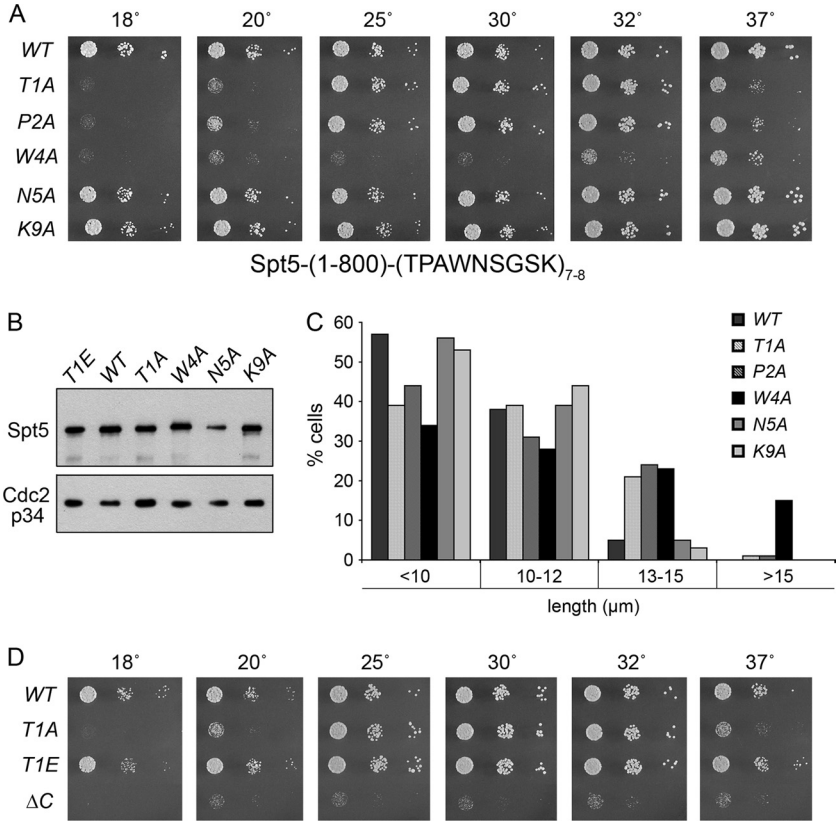

FIG. 4. Effects of alanine substitutions in the Spt5 CTD. (A) *S. pombe* strains with the indicated chromosomal *spt5-(1-800)-CTD* alleles—in which 7 or 8 wild-type or mutated CTD nonamer repeats were fused to Spt5-(1-800)—were grown in liquid medium until the A_{600} reached 0.3 to 0.5. The cultures were adjusted to equalize the A_{600}, and aliquots of serial 5-fold dilutions were spotted on YES agar medium. The plates were photographed after incubation for 8 days at 18°C, 5 days at 20°C, 3 days at 25 and 37°C, or 2 days at 30 and 32°C. WT, wild type. (B) Western blot analysis of Spt5. Whole-cell extracts of the indicated *spt5-CTD* strains were resolved by SDS-PAGE. The polypeptides were transferred to a membrane and probed by serial Western blotting with affinity-purified polyclonal anti-Spt5 antibody (top panel) and then with anti-Cdc2-p34 (PSTAIRE) antibody as a loading control (bottom panel). (C) Morphological phenotypes of *spt5-CTD* mutants. Cultures of the indicated *spt5-CTD* mutant strains were grown to mid-logarithmic phase at 30°C, and 300 to 500 individual cells were measured and sorted into the length bins specified. The percentage of cells in each bin is represented in the bar graph. (D) Effects of a phosphomimetic *T1E* change. Aliquots (3 μl) of serial 5-fold dilutions from exponentially growing cultures of the indicated strains were spotted onto YES agar medium. The plates were photographed after incubation for 8 days at 18°C, 6 days at 20°C, or 2.5 days at 30, 34, and 37°C.

and synthetic sickness suggest that the C-terminal repeat domains of Rpb1 and Spt5 overlap functionally.

Alanine scanning of the Spt5 TPAWNSGSK nonamer: effects on growth and morphology. To dissect the requirements for individual residues within the consensus repeat sequence $T^1P^2A^3W^4N^5S^6G^7S^8K^9$, we mutated the chromosomal *spt5* locus by replacing Thr1, Pro2, Trp4, Asn5, or Lys9 with alanine in each of 7 or 8 consecutive nonamer repeats that were fused to the C terminus of Spt5-(1-800) (Fig. 4A). Adding seven repeats of the wild type consensus sequence TPAWNSGSK to Spt5-(1-800) served as the positive control, insofar as the resulting *spt5-(CTD)*$_7$ "wild-type" strain grew as well as *spt5*$^+$ at all temperatures tested (Fig. 4; see also Fig. 7). Analysis of the *CTD-Ala* mutants showed that *spt5-(N5A)*$_8$ and *spt5-(K9A)*$_7$ formed wild-type-size colonies at all temperatures (Fig. 4A). In contrast, the *spt5-(W4A)*$_8$ phenotype mirrored that of *spt5-ΔC* with respect to slow growth and cold sensitivity (Fig. 4A and D), signifying that single Trp-to-Ala mutations eliminated virtually all beneficial effects of the CTD on Spt5 function *in vivo*. *spt5-(T1A)*$_7$ and *spt5-(P2A)*$_7$ cells grew as well as wild-type cells at 25, 30, and 32°C but were slower growing at 37°C and formed only tiny colonies at 18 to 20°C (Fig. 4A and D). Thus, the *T1A* and *P2A* mutations were much milder than *ΔC* and *W4A* with respect to cell growth. Thr1 is the site of phosphorylation of the Spt5 CTD by the Cdk9/Pch1 kinase (33); the adjacent Pro2 completes the (S/T)P recognition motif for cyclin-dependent kinases. The finding of concordantly diminished CTD function at restrictive temperatures in *T1A* and *P2A* mutants suggests that defective CTD phosphorylation might underlie the observed growth defects. Note that the Spt5-CTD mutant variants were expressed to comparable levels as judged by Western blot analysis (Fig. 4B and other data not shown).

We compared the cell size distributions of *spt5-CTD-Ala* mutants grown at 30°C in rich medium (Fig. 4C). Whereas *spt5-(N5A)*$_8$ and *spt5-(K9A)*$_7$ cells resembled *spt5-(CTD)*$_7$ and only 3 to 5% were 13 to 15 μm long, the fractions of *spt5-(T1A)*$_7$, *spt5-(P2A)*$_7$, and *spt5-(W4A)*$_8$ cells that were 13 to 15 μm long were 21, 24, and 23%, respectively (Fig. 4C). Only *spt5-(W4A)*$_8$ had a significant population of cells that were >15

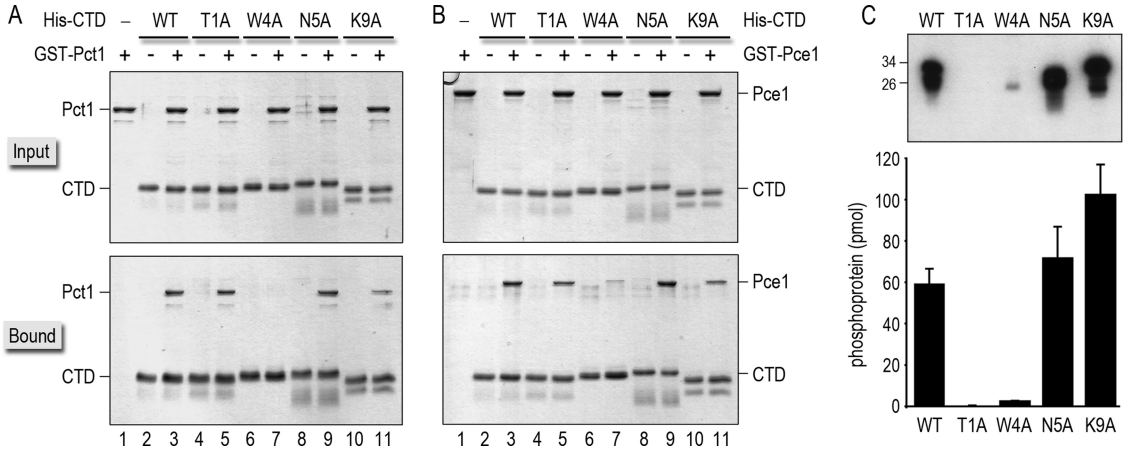

FIG. 5. Effects of Spt5 CTD-Ala mutations on binding to capping enzymes and on CTD phosphorylation by Cdk9. (A and B) Binding of GST-tagged Pct1 (A) or Pce1 (B) to wild-type and Ala-substituted His_{10}-Smt3-Spt5-CTD proteins was assessed by Ni-agarose affinity chromatography as described in Materials and Methods. The input proteins are specified above the lanes by "+." Aliquots comprising 10% of the input material (top panels) and 30% of the bead-bound material (bottom panels) were analyzed by SDS-PAGE. Polypeptides were visualized by staining the gels with Coomassie blue dye. (C) Kinase reaction mixtures (20 μl) containing 50 mM Tris acetate (pH 6.0), 1 mM DTT, 2.5 mM $MnCl_2$, 50 μM [γ^{32}P]ATP, ~100 ng of recombinant $Cdk9^{T212E}$/Pch1 kinase (36), and 1 μg of recombinant His_{10}-Smt3-Spt5-CTD phosphoacceptor as specified were incubated for 1 h at 20°C. The reactions were quenched by adding SDS to a 1% final concentration. Aliquots (3 μl) of the reaction mixtures were then analyzed by 12% SDS-PAGE. The ^{32}P-labeled proteins were visualized by autoradiography of the dried gel (top panel). The positions and sizes (kDa) of marker polypeptides are indicated on the left. The extents of label transfer from [γ^{32}P]ATP to His_{10}-Smt3-Spt5-CTD were quantified by scanning the gel with a Molecular Dynamics Typhoon PhosphorImager. The data were normalized to the initial reaction volume and are plotted as a bar graph in the bottom panel. Each datum is the average of results from three or four separate experiments ± SD.

μm long (Fig. 4C) and aberrantly branched cells (data not shown). Overexpression of Mce1, which suppressed the growth defect of *spt5-ΔC* cells, also reversed the slow-growth phenotype of *spt4-(W4A)$_8$* cells at 25, 30, and 32°C (not shown). However, Mce1 overexpression did not relieve the cold sensitivity of *spt5-(T1A)$_7$* cells (not shown).

Effects of Spt5-CTD-Ala mutations on interaction with fission yeast capping enzymes. To illuminate the basis for the phenotypes of *spt5-CTD-Ala* mutants, we queried their effects on binding to Pct1 and Pce1. Recombinant GST-Pct1 and GST-Pce1 proteins were produced in bacteria and purified from soluble lysates by affinity chromatography. The Spt5-CTD proteins were produced in bacteria as N-terminal His_{10}-Smt3 fusions. Whereas the recombinant wild-type, T1A, W4A, N5A, and K9A CTDs were readily isolated from soluble lysates by Ni^{2+} affinity chromatography, the P2A mutant was intractably insoluble and therefore not amenable to biochemical study. To assay CTD-capping enzyme interactions, the recombinant Pct1 and Pce1 proteins were mixed with the wild-type or mutant His_{10}-Smt3-Spt5-CTD proteins and then adsorbed to Ni-agarose beads. The beads were recovered and washed extensively before the bound proteins were eluted with 0.5 M imidazole. The input and bound polypeptides were then analyzed by SDS-PAGE (Fig. 5A and B). Whereas each of the His_{10}-Smt3-Spt5-CTD proteins was absorbed to the Ni-agarose resin via the His_{10} tag (lanes 2 to 11), the GST-tagged Pct1 and Pce1 proteins *per se* did not bind to Ni-agarose (lanes 1). However, when mixed with wild-type His_{10}-Smt3-Spt5-CTD, Pct1 and Pce1 were recovered in the bound fraction (lanes 3). Pct1 and Pce1 bound to the T1A and N5A CTD mutants (lanes 5 and 9). They also bound to the K9A mutant, though their extents of binding to the K9A mutant were consistently lower than those to the other CTDs (lane 11). The instructive findings were as follows: (i) no Pct1 was recovered in the bound fraction when incubated with the W4A mutant (Fig. 5A, lane 7), and (ii) only a trace amount of Pce1 bound to the W4A mutant CTD versus the wild-type CTD (Fig, 5B, lane 7). These findings, together with those in the preceding section, suggest the following: (i) that impaired Spt5-capping enzyme interactions account for, or contribute to, the observed growth defect of *spt5-(W4A)$_8$* cells (an idea consistent with the rescue of the *spt5-(W4A)$_8$* growth defect by Mce1 overexpression) and (ii) the conditional growth defects of *spt5-(T1A)$_7$* and *spt5-(P2A)$_7$* cells have other causes.

Mutational effects on Spt5 CTD phosphorylation by Cdk9. The Spt5 CTD is a substrate for threonine phosphorylation by *S. pombe* Cdk9/Pch1 (33, 49). The Cdk9 kinase is regulated by the *S. pombe* Cdk-activating kinase Csk1, which phosphorylates Cdk9 on Thr212 (36). The phosphomimetic mutant $Cdk9^{T212E}$ is activated constitutively (33, 36). Here we assessed the primary structure requirements for Spt5 phosphorylation by reacting recombinant wild-type and alanine-substituted His_{10}-Smt3-Spt5-CTD proteins (1 μg; ~50 pmol) with recombinant $Cdk9^{T212E}$/Pch1 kinase and [γ^{32}P]ATP. The reaction products were analyzed by SDS-PAGE, and the extents of ^{32}P label transfer to the Spt5 CTD phosphoacceptors were quantified (Fig. 5C). Whereas 60 pmol of $^{32}P_i$ was incorporated into the wild-type CTD, we detected no label transfer to the T1A CTD mutant (Fig. 5C). This result confirms previous inferences from phosphoamino acid analysis (33) that Thr1 is the direct target for Cdk9 phosphorylation. The N5A and K9A mutants were as good or better as substrates for Cdk9 than wild-type Spt5 CTD (Fig. 5C), consistent with the benign effect of the N5A and K9A changes on Spt5 activity *in vivo*. In contrast, the W4A mutation reduced the extent of CTD phosphorylation by a factor of 20 (Fig. 5C). The fact that Trp4 is

critical for all aspects of Spt5 CTD function tested (cell growth and morphology, capping enzyme binding, and phosphorylation by Cdk9) implies that Trp4 is essential for proper folding of the Spt5 CTD, whether it be intrinsic to the CTD or templated by proteins that interact with the CTD.

Threonine-to-glutamate substitutions in the Spt5 CTD. We replaced the chromosomal *spt5*$^+$ locus with a *T1E* mutant in which Thr1 was changed to glutamate (a phosphomimetic) in each of 7 nonamer repeats fused to Spt5-(1-800). The *spt5-(T1E)*$_7$ cells grew as well as wild-type *spt5-(CTD)*$_7$ cells at all temperatures tested (Fig. 4D), and they also displayed wild-type morphology (not shown). These findings contrast with the cold-sensitive growth defect and modestly elongated shape of the *spt5-(T1A)*$_7$ mutant (Fig. 4C and D). We surmise that Thr1 phosphorylation of the Spt5 CTD is important *in vivo* and there is no obvious penalty to a constitutive phosphomimetic state.

Spt5 CTD T1A and P2A mutations confer sensitivity to 6-azauracil. The ribonucleotide-depleting drug 6-azauracil (6-AU) slows the growth of yeast strains carrying mutations in genes that encode proteins involved in transcription elongation (3, 28, 43, 46). To determine whether *spt5-CTD-Ala* mutant strains are sensitive to 6-AU, we tested their growth on agar plates containing 0, 200, or 300 μg/ml 6-AU (Fig. 6). In parallel, we assessed the effect of 6-AU on growth of cells carrying the *spt5-CTD-Ala rpb1-16* and *spt5-CTD-Ala rpb1-12* alleles (Fig. 6). The *spt5-(N5A)*$_8$ and *spt5-(T1E)*$_7$ mutants grew comparably to the *spt5-(CTD)*$_7$ strain in the *rpb1*$^+$, *rpb1-16*, and *rpb1-12* strain backgrounds. In contrast, the CTD *T1A* and *P2A* mutations sensitized *S. pombe* to 300 μg/ml 6-AU in the *rpb1*$^+$ background, resulting in slowed growth (Fig. 6, top panels). Whereas truncating the Rpb1 CTD to 16 and 12 heptad repeats had little or no effect on 6-AU sensitivity *per se*, the *rpb1-16* and *rpb1-12* alleles progressively exacerbated the 6-AU sensitivity of the *spt5-(T1A)*$_7$ and *spt5-(P2A)*$_7$ mutants (Fig. 6, middle and bottom panels). The distinctive effects of Thr1 and Pro2 mutations on 6-AU sensitivity imply a positive role for Spt5 CTD phosphorylation in transcription elongation in fission yeast.

Combining Pol II CTD Ser2 and Spt5 CTD Thr1 mutations. *S. pombe* Cdk9 catalyzes threonine phosphorylation of the Spt5 CTD and serine phosphorylation of the Pol II CTD (33). Probing of the Cdk9-phosphorylated Pol II CTD product with various antibodies suggested that Cdk9 acts on Ser2 and Ser5 of the YSPTSPS heptad (13, 36). Most of the bulk Ser2 phosphorylation of the fission yeast Rpb1 CTD *in vivo* depends on a different nonessential Cdk enzyme named Lsk1 (23). Nonetheless, a fraction of Rpb1 Ser2 phosphorylation *in vivo* appears to require Cdk9, as inferred from experiments with analog-sensitive kinase mutants (49). The finding that a mutated Rpb1 CTD in which Ser2 was replaced by alanine could sustain *S. pombe* viability, albeit with conditional defects in cytokinesis (23), had two important ramifications: (i) that Ser2 phosphorylation is not globally essential for Pol II transcription and (ii) that the essentiality of the *S. pombe* Cdk9 kinase (36) reflects its phosphorylation of a critical target other than Rpb1 CTD-Ser2. One obvious candidate is the Spt5 CTD Thr1, which, though also not essential, might overlap functionally with Rpb1 Ser2. To evaluate this scenario, we tested for mutational synergy between an Rpb1 CTD-S2A mutation and an Spt5 CTD T1A mutation.

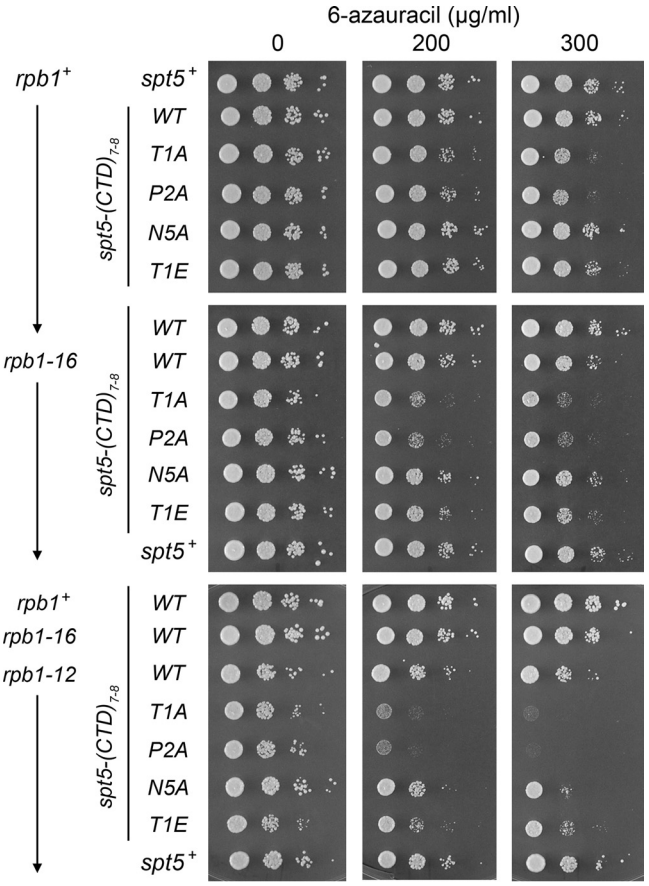

FIG. 6. Spt5 CTD *T1A* and *P2A* mutations sensitize fission yeast to growth inhibition by 6-azauracil. Exponentially growing cultures of *S. pombe* strains with the indicated *rbp1* and *spt5* genotypes were adjusted to an A_{600} of 0.1, and aliquots (3 μl) of serial 5-fold dilutions were spotted on synthetic agar medium lacking uracil and containing 6 mM NH_4OH and 0, 200, or 300 μg/ml 6-azauracil (6-AU) as specified. The plates were incubated at 30°C for 4 days (no 6-AU), 5 days (200 μg/ml 6-AU), or 5.5 days (300 μg/ml 6-AU).

We constructed an *rpb1-S2A* allele that encodes 14 tandem repeats of the mutant heptad YAPTSPS fused to the first 4 imperfect heptad variants of the wild-type Rpb1 subunit (Fig. 7). Our version of S2A has two more mutant heptads than that described previously (23). The haploid *S. pombe rpb1-S2A* strain grew as well as the *rpb1*$^+$ and *rpb1-16* (which contains a "wild type" CTD sequence of similar length) strains at 30°C but was slower growing at 25°C and extremely sick at 20 and 37°C (Fig. 7, bottom panels).

To assay mutational synergy, we combined the *rpb1-S2A* allele with *spt5-(CTD)*$_7$, *spt5-(T1A)*$_7$, and *spt5-(T1E)*$_7$. The relevant findings were as follows: (i) truncating the Spt5 CTD to 7 "wild type" nonamer repeats (which had no effect in an *rpb1-16* background) exacerbated the *rpb1-S2A* cold-sensitive phenotype (see results for 20°C); (ii) there was no synthetic growth defect for the *rpb1-S2A spt5-(T1A)*$_7$ double mutant; (iii) the constitutive Spt5 phosphomimetic *spt5-(T1E)*$_7$ mutation did not suppress the conditional growth defects of *rpb1-S2A* (Fig. 7). We surmise that phosphorylations of Rpb1 Ser2

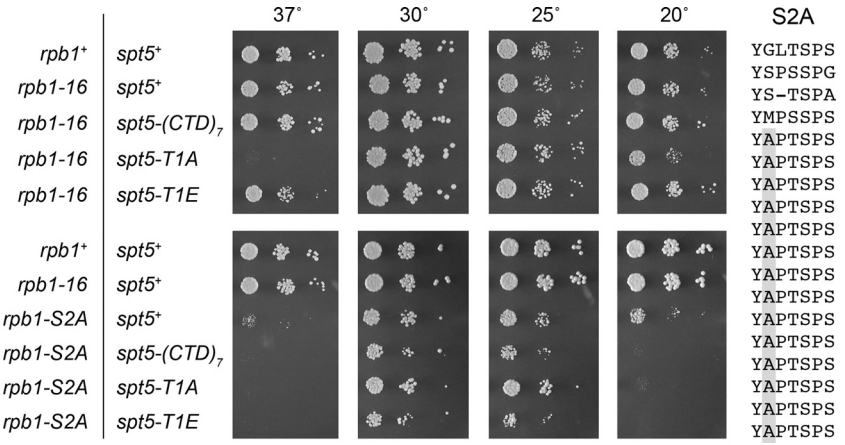

FIG. 7. Effects of *spt5-CTD* mutations in combination with *rpb1-S2A*. The amino acid sequence of the *S. pombe* Rpb1 CTD-S2A variant is shown at right. The heptapeptide repeats are stacked vertically with the mutated Ser2 positions shaded in gray. The indicated fission yeast strains were maintained in logarithmic growth at 30°C in YES medium. The cultures were adjusted to an A_{600} of 0.01, and aliquots of 10-fold serial dilutions were spotted on YES agar medium. The genotypes of the strains with respect to the *rpb1* and *spt5* loci are indicated on the left. The plates shown in the upper panels were incubated for either 2 days at 37 and 30°C, 3 days at 25°C, or 5 days at 20°C. The plates shown in the lower panels were incubated for either 2 days at 37 and 30°C, 4 days at 25°C, or 7 days at 20°C.

and/or Spt5 Thr1 are not essential for viability of *S. pombe* and that Cdk9 phosphorylates another essential target site *in vivo*.

DISCUSSION

The Spt5 and Pol II CTDs perform overlapping essential functions. We show here that the CTD nonamer repeat array of fission yeast Spt5 is important for normal physiology, insofar as its complete deletion elicits a constitutive slow-growth defect and aberrant cell morphology. The *spt5-ΔC* phenotype is mimicked by replacing Trp4 in each TPAWNSGSK nonapeptide with alanine, which attests to a likely structural role for this defining residue of the *S. pombe* Spt5 CTD. The Spt5 homologs of other eukarya also have CTD arrays with repeating (Thr/Ser)Pro motifs, albeit less regular in their spacing and primary structure than that of *S. pombe* (32). In particular, whereas the residue located two positions downstream of the Thr-Pro dipeptide in *S. pombe* Spt5 is a tryptophan in 12 of the CTD repeats (Fig. 2), it is never a tryptophan in the human, nematode, or zebra fish proteins. The Spt5 CTD of budding yeast *S. cerevisiae* is atypical in that it contains 15 tandem repeats of a proline-free hexapeptide motif of the consensus sequence S(A/T)WGG(A/Q), in which the first serine residue is a substrate for phosphorylation by the cyclin-dependent Bur1 kinase (26, 58). Budding yeast Bur1 is the ortholog of fission yeast Cdk9 (33, 35). Immediately upstream of this CTD hexapeptide array in *S. cerevisiae* Spt5 is a pair of Thr-Pro dipeptides, each of which is embedded in a short motif—^{905}TPGWSS and ^{916}TPAVNA—that bears some similarity to the *S. pombe* Spt5 CTD repeat unit. Probing of cell extracts with phosphoamino acid antibodies suggested that *S. cerevisiae* Spt5 contains phosphothreonine (58), though the threonine phosphorylation sites were not identified.

Notwithstanding these differences in CTD structure, there is an emerging consensus from genetic studies that the Spt5 CTD plays an important, but not strictly essential, role in Spt5 function *in vivo*. To wit, whereas knockdown of human Spt5 blocked proliferation of HeLa cells, cell growth was restored by a human Spt5 mutant lacking the CTD repeat module (24). This result prompted speculation of functional redundancy of the human Spt5 CTD. Deletion of the hexapeptide CTD repeat array of *S. cerevisiae* Spt5 had no effect on cell growth at 30°C but resulted in slow growth at 16°C (26) and sensitivity to 6-AU (58). (Note that the *spt5-ΔCTD* growth phenotype in budding yeast is less severe than that in *S. pombe* and appears more akin to the effects of the *S. pombe spt5-T1A* mutant.)

To explore the potential functional redundancies of the *S. pombe* Spt5 CTD, we focused on the Rbp1 CTD heptad array, reasoning that because both CTDs bind proteins that act cotranscriptionally and receive inputs via phosphorylation of their component repeats, the presence of one of the CTDs might buffer the loss or truncation of the other CTD. Here we conducted the first incremental deletion analysis of the *S. pombe* Rpb1 CTD, which revealed the following: (i) 16 of the 29 heptad repeats are needed for wild-type growth on standard medium; (ii) less than 10 heptads is constitutively lethal; and (iii) serial trimmings between 13 and 10 heptads progressively worsen cell growth. Two prior studies had each documented a single viable *S. pombe rpb1-ΔCTD* allele, though their nomenclatures differed from each other and from ours with respect to heptad counting. By reference to the heptad alignment in Fig. 2, the viable but slow-growing *rpb1-11* allele in the work of Schramke et al. (40) contained 12 repeats, and the *rpb1-12xCTD* allele of Karagiannis and Balasubramanian (23) contained 16 repeats.

A key finding of our study is that the otherwise viable CTD truncation mutations *rpb1-11*, *-12*, and *-13* are synthetic lethal with *spt5-ΔC*, while *rpb-16* and *spt5-ΔC* are synthetically very sick. Even a modest shortening of the Pol II CTD to 20 repeats exacerbated the *spt5-ΔC* growth defect. These results provide evidence for an essential overlapping function(s) of the Spt5 and Pol II CTDs in fission yeast. Similar inferences were drawn for budding yeast based on the observation that the viable *spt5-ΔCTD* allele was synthetic lethal with a viable *ctk1Δ* null

allele that lacks the major yeast Rbp1 CTD-Ser2 kinase Ctk1 (26), a result taken to mean that Pol II Ser2 phosphorylation and Spt5 CTD phosphorylation are the functionally overlapping principles. However, this scenario cannot pertain in fission yeast, where we see no synergy between an *spt5-T1A* mutation that eliminates the Spt5 CTD phosphorylation site and an *rpb1-S2A* mutation.

Fortifying the CTD connection to capping enzymes in *S. pombe*. The fission yeast capping enzymes RNA triphosphatase (Pct1) and RNA guanylyltransferase (Pce1) are separately encoded essential proteins that bind independently to the phosphorylated Rbp1 CTD heptad array and to the unphosphorylated *S. pombe* Spt5 CTD nonamer array (32, 34). The mammalian capping enzyme Mce1 is a single modular polypeptide composed of N-terminal triphosphatase and C-terminal guanylyltransferase domains. The Mce1 guanylyltransferase domain binds to the phosphorylated Pol II CTD and thereby ferries the covalently tethered triphosphatase module, which does not bind to the Pol II CTD on its own, to the mammalian Pol II elongation complex (18, 19). Both isolated domains of Mce1 can bind to human Spt5 via its CTD, and this interaction increases the efficiency of contranscriptional capping, especially when the Pol II CTD is in the dephosphorylated state (27, 52). It is noteworthy that Mce1 does not bind to the *S. pombe* Spt5 CTD (32). Our finding here that Mce1 is a dosage suppressor of the growth defect and elongated shape of the *spt5-ΔC* mutant attests that capping enzyme recruitment is likely a limiting factor in the absence of the Spt5 CTD. Overexpression of Mce1, or combined overexpression of Pct1 and Pce1, presumably drives their binding directly to the phosphorylated Rbp1 CTD, either by simple mass action or by competition with other cellular CTD-binding proteins. An appealing scenario, admittedly speculative at this stage, is that the fission yeast triphosphatase and guanylyltransferase bind initially to the unphosphorylated Spt5 CTD and are then handed off to the nearby Poll II CTD within the same transcription complex after Rbp1 is phosphorylated on Ser5. It is noteworthy that capping enzyme overexpression does not alleviate the slow growth of *spt5-ΔC* cells at low temperatures, indicating that the Spt5 CTD has other functions beyond capping.

A genetically separable contribution of Spt5 to transcription elongation relies on threonine phosphorylation. Replacing the Spt5 CTD Thr1 side chain with alanine abolished its ability to serve as a phosphoacceptor substrate for Cdk9 without impacting the interactions with the capping enzymes Pct1 and Pce1. The *T1A* mutation elicited a milder phenotype *in vivo* than did complete deletion of the Spt5 CTD, said phenotype comprising cold-sensitive (cs) and temperature-sensitive (ts) growth (that was unaffected by Mce1 overexpression) and sensitivity to growth inhibition by 6-AU. The cs and ts growth and 6-AU sensitivity are both suppressed by the phosphomimetic *T1E* change, thereby implicating deficient Spt5 CTD phosphorylation as the culprit in a putative transcription elongation abnormality in *T1A* cells. 6-AU sensitivity of *T1A* cells was enhanced by shortening the Pol II CTD to 16 heptad repeats, though the *rpb1-16* allele itself caused no 6-AU sensitivity. This trend progressed as *spt5-T1A* was combined with the *rpb1-12* allele. We surmise from these results that the Pol II CTD and the threonine-phosphorylated Spt5 CTD play overlapping positive roles in elongation. However, as noted above, the overlap is not at the level of Ser2 phosphorylation of the Rpb1 CTD array, because there was no synergy between *rpb1-S2A* and *spt5-T1A*, as gauged by growth on standard medium. We thereby infer the existence of at least one additional critical target for the essential Cdk9 kinase. Conceivably, Cdk9 could phosphorylate a different position within the Rbp1 CTD heptad (Ser5 and/or Ser7) or yet another protein involved in transcriptional control in fission yeast. *S. pombe* Cdk9 can phosphorylate Rpb1 on Ser5 *in vitro* (36), and it is appealing to think that Cdk9 phosphorylation of Ser5, coordinated temporally (during the transcription cycle) and spatially (within the linear heptad array) with Cdk7's Ser5 phosphorylation function, might comprise an internal "CTD clock," analogous to recent discussions of how Cdk7 Ser5 phosphorylation primes subsequent CTD phosphorylations of Ser2 (38, 49).

ACKNOWLEDGMENTS

This work was supported by National Institutes of Health grant GM52470. S.S. is an American Cancer Society Research Professor.

REFERENCES

1. **Akhtar, M. S., M. Heidermann, J. R. Tietjen, D. W. Zhang, R. D. Chapman, D. Eick, and A. Z. Ansari.** 2009. TFIIH kinase places bivalent marks on the carboxy-terminal domain of RNA polymerase II. Mol. Cell **34:**387–393.
2. **Andrulis, E. D., E. Guzman, P. Dumloring, J. Werner, and J. T. Lis.** 2000. High-resolution localization of *Drosophila* Spt5 and Spt6 at heat shock genes *in vivo*: roles in promoter proximal pausing and transcription elongation. Genes Dev. **14:**2635–2649.
3. **Archambault, J., F. LaCroute, A. Ruet, and J. D. Friesen.** 1992. Genetic interaction between transcription elongation factor TFIIS and RNA polymerase II. Mol. Cell. Biol. **12:**4142–4152.
4. **Azuma, Y., M. Yamagashi, R. Ueshima, and A. Ishihama.** 1991. Cloning and sequence determination of the *Schizosaccharomyces pombe rpb1* gene encoding the largest subunit of RNA polymerase II. Nucleic Acids Res. **19:**461–468.
5. **Chen, Y., Y. Yamaguchi, Y. Tsugeno, J. Yamamoto, T. Yamada, M. Nakamura, K. Hisatake, and H. Handa.** 2009. DISF, the Paf1 complex, and Tat-SF1 have nonredundant, cooperative roles in RNA polymerase II elongation. Genes Dev. **23:**2765–2777.
6. **Chiu, Y. L., C. K. Ho, N. Saha, B. Schwer, S. Shuman, and T. M. Rana.** 2002. Tat stimulates cotranscriptional capping of HIV mRNA. Mol. Cell **10:**585–597.
7. **Cho, E., T. Takagi, C. R. Moore, and S. Buratowski.** 1997. mRNA capping enzyme is recruited to the transcription complex by phosphorylation of the RNA polymerase II carboxyl-terminal domain. Genes Dev. **11:**3319–3326.
8. **Fabrega, C., V. Shen, S. Shuman, and C. D. Lima.** 2003. Structure of an mRNA capping enzyme bound to the phosphorylated carboxyl-terminal domain of RNA polymerase II. Mol. Cell **11:**1549–1561.
9. **Forsburg, S. L.** 1993. Comparison of *Schizosaccharomyces pombe* expression systems. Nucleic Acids Res. **21:**2955–2956.
10. **Forsburg, S. L., and D. A. Sherman.** 1997. General purpose tagging vectors for fission yeast. Gene **191:**191–195.
11. **Forsburg, S. L., and N. Rhind.** 2006. Basic methods for fission yeast. Yeast **23:**173–183.
12. **Gao, L., and D. S. Gross.** 2008. Sir2 silences gene transcription by targeting the transition between RNA polymerase II initiation and elongation. Mol. Cell. Biol. **28:**3979–3994.
13. **Guiguen, A., J. Soutourine, M. Dewez, L. Tafforeau, M. Dieu, M. Raes, J. Vandenhaute, M. Werner, and D. Hermand.** 2007. Recruitment of P-TEFb (Cdk9-Pch1) to chromatin by the cap-methyl transferase Pcm1 in fission yeast. EMBO J. **26:**1552–1559.
14. **Guo, M., F. Xu, J. Yamada, T. Egelhofer, Y. Gao, G. A. Hartzog, M. Teng, and L. Niu.** 2008. Core structure of the yeast Spt4-Spt5 complex: a conserved module for regulation of transcription elongation. Structure **16:**1649–1658.
15. **Hagler, J., and S. Shuman.** 1992. A freeze-frame view of eukaryotic transcription during elongation and capping of nascent mRNA. Science **255:**983–986.
16. **Hartzog, G. A., M. A. Basrai, S. L. Ricupero-Hovasse, P. Hieter, and F. Winston.** 1996. Identification and analysis of a functional human homolog of the *SPT4* gene of *Saccharomyces cerevisiae*. Mol. Cell. Biol. **16:**2848–2856.
17. **Hartzog, G. A., T. Wada, H. Handa, and F. Winston.** 1998. Evidence that Spt4, Spt5 and Spt6 control transcription elongation by RNA polymerase II in *Saccharomyces cerevisiae*. Genes Dev. **12:**357–369.
18. **Ho, C. K., and S. Shuman.** 1999. Distinct roles for CTD Ser2 and Ser5

phosphorylation in the recruitment and allosteric activation of mammalian capping enzyme. Mol. Cell **3:**405–411.
19. **Ho, C. K., V. Sriskanda, S. McCracken, D. Bentley, B. Schwer, and S. Shuman.** 1998. The guanylyltransferase domain of mammalian mRNA capping enzyme binds to the phosphorylated carboxyl-terminal domain of RNA polymerase II. J. Biol. Chem. **273:**9577–9585.
20. **Hong, S. W., S. M. Hong, J. W. Yoo, Y. C. Lee, S. Kim, J. T. Lis, and D. Kee.** 2009. Phosphorylation of the RNA polymerase II C-terminal domain by TFIIH kinase is not essential for transcription of *Saccharomyces cerevisiae* genome. Proc. Natl. Acad. Sci. U. S. A. **106:**14276–14280.
21. **Jennings, B. H., S. Shah, Y. Yamaguchi, M. Seki, R. G. Phillips, H. Handa, and D. Ish-Horowicz.** 2004. Locus-specific requirements for Spt5 in transcriptional activation and repression in *Drosophila*. Curr. Biol. **14:**1680–1684.
22. **Kanin, E. I., R. T. Kipp, C. Kung, M. Slattery, A. Viale, S. Hahn, K. M. Shokat, and A. Z. Ansari.** 2007. Chemical inhibition of the THIIH-associated kinase Cdk7/Kin28 does not impair global mRNA synthesis. Proc. Natl. Acad. Sci. U. S. A. **104:**5812–5817.
23. **Karagiannis, J., and M. K. Balasubramanian.** 2007. A cyclin-dependent kinase that promotes cytokinesis through modulating phosphorylation of the carboxy terminal domain of the RNA Pol II Rpb1p subunit. PLoS One **2:**e433.
24. **Komori, T., N. Inukai, T. Yamada, Y. Yamaguchi, and H. Handa.** 2009. Role of human transcription elongation factor DSIF in the suppression of senescence and apoptosis. Genes Cells **14:**343–354.
25. **Krishnan, K., N. Salomonis, and S. Guo.** 2008. Identification of Spt5 target genes in zebrafish development reveals its dual activity *in vivo*. PLoS One **3:**e3621.
26. **Liu, Y., L. Warfield, C. Zhang, J. Luo, J. Allen, W. H. Lang, J. Ranish, K. M. Shokat, and S. Hahn.** 2009. Phosphorylation of the transcription factor Spt5 by yeast Bur1 kinase stimulates recruitment of the PAF complex. Mol. Cell. Biol. **29:**4852–4963.
27. **Mandal, S. S., C. Chu, T. Wada, H. Handa, A. J. Shatkin, and D. Reinberg.** 2004. Functional interaction of RNA-capping enzyme with factors that positively and negatively regulate promoter escape by RNA polymerase II. Proc. Natl. Acad. Sci. U. S. A. **101:**7572–7577.
28. **Mason, P. B., and K. Struhl.** 2005. Distinction and relationship between elongation rate and processivity of RNA polymerase II *in vivo*. Mol. Cell **17:**831–840.
29. **McCracken, S., N. Fong, E. Rosonina, K. Yankulov, G. Brothers, D. Siderovski, A. Hessel, S. Foster, S. Shuman, and D. L. Bentley.** 1997. 5′ Capping enzymes are targeted to pre-mRNA by binding to the phosphorylated C-terminal domain of RNA polymerase II. Genes Dev. **11:**3306–3318.
30. **Meinhart, A., T. Kamenski, S. Hoeppner, S. Baumli, and P. Cramer.** 2005. A structural perspective of CTD function. Genes Dev. **19:**1401–1415.
31. **Nonet, M., D. Sweetser, and R. A. Young.** 1987. Functional redundancy and structural polymorphism in the large subunit of RNA polymerase II. Cell **50:**909–915.
32. **Pei, Y., and S. Shuman.** 2002. Interactions between fission yeast mRNA capping enzymes and elongation factor Spt5. J. Biol. Chem. **277:**19639–19648.
33. **Pei, Y., and S. Shuman.** 2003. Characterization of the *Schizosaccharomyces pombe* Cdk9/Pch1 protein kinase: Spt5 phosphorylation, autophosphorylation and mutational analysis. J. Biol. Chem. **278:**43346–43356.
34. **Pei, Y., S. Hausmann, C. K. Ho, B. Schwer, and S. Shuman.** 2001. The length, phosphorylation state, and primary structure of the RNA polymerase II carboxyl-terminal domain dictate interactions with mRNA capping enzymes. J. Biol. Chem. **276:**28075–28082.
35. **Pei, Y., B. Schwer, and S. Shuman.** 2003. Interactions between fission yeast Cdk9, its cyclin partner Pch1, and mRNA capping enzyme Pct1 suggest an elongation checkpoint for mRNA quality control. J. Biol. Chem. **278:**7180–7188.
36. **Pei, Y., H. Du, J. Singer, St. C. Amour, S. Granitto, S. Shuman, and R. P. Fisher.** 2006. Cdk9 of fission yeast is activated by the CDK-activating kinase Csk1, overlaps functionally with the TFIIH-associated kinase Mcs6, and associates with the cap methyltransferase Pcm1 *in vivo*. Mol. Cell. Biol. **26:**777–788.
37. **Phatnani, H. P., and A. L. Greenleaf.** 2006. Phosphorylation and functions of the RNA polymerase II CTD. Genes Dev. **20:**2922–2936.
38. **Qiu, H., C. Hu, and A. G. Hinnebusch.** 2009. Phosphorylation of the Pol II CTD by KIN29 enhances BUR1/BUR2 recruitment and Ser2 CTD phosphorylation near promoters. Mol. Cell **33:**752–762.
39. **Renner, D. B., Y. Yamaguchi, T. Wada, H. Handa, and D. H. Price.** 2001. A highly purified RNA polymerase II elongation control system. J. Biol. Chem. **276:**42601–42609.
40. **Schramke, V., D. M. Sheedy, A. M. Denli, C. Bonila, K. Ekwall, G. J. Hannon, and R. C. Allshire.** 2005. RNA-interference-directed chromatin modification coupled to RNA polymerase II transcription. Nature **435:**1275–1279.
41. **Schwer, B., X. Mao, and S. Shuman.** 1998. Accelerated mRNA decay in conditional mutants of yeast mRNA capping enzyme. Nucleic Acids Res. **26:**2050–2057.
42. **Schwer, B., S. Schneider, Y. Pei, A. Aronova, and S. Shuman.** 2009. Characterization of the *Schizosaccharomyces pombe* Spt5-Spt4 complex. RNA. **15:**1241–1250.
43. **Shaw, R. J., and D. Reines.** 2000. *Saccharomyces cerevisiae* transcription elongation mutants are defective in *PUR5* induction in response to nucleotide depletion. Mol. Cell. Biol. **20:**7427–7437.
44. **Shim, E. Y., A. K. Walker, Y. Shi, and K. T. Blackwell.** 2002. CDK-9/cyclin T (P-TEFb) is required in two postinitiation pathways for transcription in the *C. elegans* embryo. Genes Dev. **16:**2135–2146.
45. **Sims, R. J., R. Belotserkovskaya, and D. Reinberg.** 2004. Elongation by RNA polymerase II: the short and long of it. Genes Dev. **18:**2437–2468.
46. **Squazzo, S. L., P. J. Costa, D. L. Lindstrom, K. E. Kumer, R. Simic, J. L. Jennings, A. J. Link, K. M. Arndt, and G. A. Hartzog.** 2002. The Paf1 complex physically and functionally associates with transcription elongation factors *in vivo*. EMBO J. **21:**1764–1774.
47. **Swanson, M. S., E. A. Malone, and F. Winston.** 1991. *SPT5*, an essential gene important for normal transcription in *Saccharomyces cerevisiae*, encodes an acidic nuclear protein with a carboxy-terminal repeat. Mol. Cell. Biol. **11:**3009–3019.
48. **Thompson, C. M., A. J. Koleske, D. M. Chao, and R. A. Young.** 1993. A multisubunit complex associated with the RNA polymerase II CTD and TATA-binding protein in yeast. Cell **73:**1361–1375.
49. **Viladevall, L., St. C. V. Amour, A. Rosebrock, S. Schneider, C. Zhang, J. J. Allen, K. M. Shokat, B. Schwer, J. K. Leatherwood, and R. P. Fisher.** 2009. TFIIH and P-TEFb coordinate transcription with capping enzyme recruitment at specific genes in fission yeast. Mol. Cell **33:**738–751.
50. **Wada, T., T. Takagi, Y. Yamaguchi, A. Ferdous, T. Imai, S. Hirose, S. Sugimoto, K. Yano, G. A. Hartzog, F. Winston, S. Buratowski, and H. Handa.** 1998. DSIF, a novel transcription elongation factor that regulates RNA polymerase II processivity, is composed of human Spt4 and Spt5 homologs. Genes Dev. **12:**343–356.
51. **Wada, T., T. Takagi, Y. Yamaguchi, D. Watanabe, and H. Handa.** 1998. Evidence that P-TEFb alleviates the negative effect of DSIF on RNA polymerase II-dependent transcription in vitro. EMBO J. **17:**7395–7403.
52. **Wen, Y., and A. J. Shatkin.** 1999. Transcription elongation factor hSpt5 stimulates mRNA capping. Genes Dev. **13:**1774–1779.
53. **Wenzel, S., B. M. Martins, P. Rörsch, and B. M. Wöhrli.** 2010. Crystal structure of the human transcription elongation factor DSIF hSpt4 subunit in complex with the hSpt5 dimerization interface. Biochem. J. **425:**373–380.
54. **West, M. L., and J. L. Corden.** 1995. Construction and analysis of yeast RNA polymerase II CTD deletion and substitution mutations. Genetics **140:**1223–1233.
55. **Wu, C. H., Y. Yamaguchi, L. R. Benjamin, M. Horvat-Gordon, J. Washinky, E. Enerly, J. Larsson, A. Lambertsson, H. Handa, and D. Gilmour.** 2003. NELF and DSIF cause promoter proximal pausing on the *hsp70* promoter in *Drosophila*. Genes Dev. **17:**1402–1414.
56. **Yamada, T., Y. Yamaguchi, N. Inukai, S. Okamoto, T. Mura, and H. Handa.** 2006. P-TEFb-mediated phosphorylation of hSpt5 C-terminal repeats is critical for processive transcription elongation. Mol. Cell **21:**227–237.
57. **Yue, Z., E. Maldonado, R. Pillutla, H. Cho, D. Reinberg, and A. J. Shatkin.** 1997. Mammalian capping enzyme complements mutant *S. cerevisiae* lacking mRNA guanylyltransferase and selectively binds the elongating form of RNA polymerase II. Proc. Natl. Acad. Sci. U. S. A. **94:**12898–12903.
58. **Zhou, K., W. H. W. Kuo, J. Fillingham, and J. F. Greenblatt.** 2009. Control of transcriptional histone modification by the yeast BUR kinase substrate Spt5. Proc. Natl. Acad. Sci. U. S. A. **106:**6956–6961.